DOI: 10.1002/chem.201101223

Aerobic Epoxidation of Olefins Catalyzed by the Cobalt-Based Metal–Organic Framework STA-12(Co)

Matthias J. Beier,[a, b] Wolfgang Kleist,*[b, c] Michael T. Wharmby,[d] Reinhard Kissner,[b] Bertram Kimmerle,[b] Paul A. Wright,[d] Jan-Dierk Grunwaldt,[a, c] and Alfons Baiker[b]

Abstract: A Co-based metal–organic framework (MOF) was investigated as a catalytic material in the aerobic epoxidation of olefins in DMF and exhibited, based on catalyst mass, a remarkably high catalytic activity compared with the Co-doped zeolite catalysts that are typically used in this reaction. The structure of STA-12(Co) is similar to that of STA-12(Ni), as shown by XRD Rietveld refinement and is stable up to 270 °C. For the epoxidation reaction, significantly different selectivities were obtained depending on the substrate. Although styrene was epoxidized with low selectivity due to oligomerization, (*E*)-stilbene was converted with high selectivities between 80 and 90 %. Leaching of Co was low and the reaction was found to proceed mainly heterogeneously. The catalyst was reusable with only a small loss of activity. The catalytic epoxidation of stilbene with the MOF featured an induction period, which was, interestingly, considerably reduced by styrene/stilbene co-epoxidation. This could be traced back to the formation of benzaldehyde promoting the reaction. Detailed parameter and catalytic studies, including in situ EPR and EXAFS spectroscopy, were performed to obtain an initial insight into the reaction mechanism.

Keywords: cobalt · epoxidation · heterogeneous catalysis · metal–organic frameworks · stilbene oxides

Introduction

Among oxidation reactions, the epoxidation of olefins plays a prominent role. Epoxides are highly reactive and therefore frequently used as intermediates in industry.[1] Ethylene oxide is one of the world's most highly demanded chemicals with production of 2.9×10^6 tons in 2008 in the US alone.[2] Ethylene oxide leads to the formation of ethylene glycols through hydrolysis[1] and thus forms the basis for many everyday products, including anti-freezing agents and cosmetics, among others. In contrast to ethylene, the (catalytic) epoxidation of more complex olefins frequently requires oxygen in an activated form.[3] As an example, isolated Ti centers in a silica matrix have been shown to be ideal heterogeneous catalysts for epoxidation reactions by using simple peroxides, such as *t*BuOOH and hydrogen peroxide.[3–5] In recent years, catalytic systems have been developed that use molecular oxygen in the liquid phase as the least expensive oxidant for epoxidation reactions. Heterogeneous gold catalysts have been reported to be catalytically active in the aerobic epoxidation of a number of olefins both with[6] and without radical initiators.[7] The formation of secondary by-products from oxygen was not reported in these cases, although other aerobic gold-based epoxidations require the activation of oxygen through an intermediate organic peroxide.[8,9] The Mukaiyama epoxidation is a general protocol that facilitates the epoxidation of an olefin with oxygen by using a sacrificial aldehyde in the presence of various transition metals.[10–12] The aldehyde is transformed in situ into a carboxylperoxo radical, facilitating oxygen transfer to the olefin. As a stoichiometric side product, the carboxylic acid is formed.

Several papers report the successful epoxidation of olefins with molecular oxygen in the absence of additional sacrificial reductants or radical initiators in DMF. Generally, heterogeneous Co catalysts were used in these investigations.[13–22] The use of amide solvents is required for catalytic activity. This is mostly interpreted in terms of the formation of a Co–DMF complex that reacts with oxygen to give a Co superoxo species which transfers oxygen to the olefin. To the best of our knowledge, only one study has reported that

[a] Dr. M. J. Beier, Prof. J.-D. Grunwaldt
Department of Chemical and Biochemical Engineering
Technical University of Denmark
DK-2800 Kgs. Lyngby (Denmark)

[b] Dr. M. J. Beier, Dr. W. Kleist, Dr. R. Kissner, Dr. B. Kimmerle, Prof. A. Baiker
Department of Chemistry and Applied Biosciences
ETH Zurich, Hönggerberg, HCI, CH-8093 Zurich (Switzerland)

[c] Dr. W. Kleist, Prof. J.-D. Grunwaldt
Institute of Catalysis Research and Technology
Karlsruhe Institute of Technology (KIT)
Herrmann-von-Helmholtz-Platz 1,
D-76344 Eggenstein-Leopoldshafen (Germany)
Fax: (+49) 721-608-44820
E-mail: wolfgang.kleist@kit.edu

[d] M. T. Wharmby, Prof. P. A. Wright
School of Chemistry, University of St. Andrews
Purdie Building, North Haugh, St Andrews,
Fife, KY16 9ST (United Kingdom)

Supporting information for this article is available on the WWW under http://dx.doi.org/10.1002/chem.201101223.

the olefin transformation is accompanied by significant DMF oxidation[23] to *N*-formyl-*N*-methylformamide (FMF), which might provide an alternative explanation of the epoxidation on the basis of a solvent co-oxidation mechanism. Based on experiments with radical scavengers, the mechanism was suggested to be of radical nature. Co-substituted zeolites turned out to be the most effective catalysts and a general conclusion was that isolated Co species are the most active. Since isolated species can only be obtained with low Co loading in zeolites, rather high absolute catalyst amounts are required.

Metal–organic frameworks (MOFs) feature, like zeolites, isolated metal centers that are well-distributed and well-defined. Several groups have reported the targeted biomimetic modification of MOFs as an additional strategy.[24,25] Their main advantage compared with zeolites consists in their substantially higher metal loading, which offers the opportunity to significantly reduce the overall amount of catalyst, provided that the internal metal centers are accessible to the substrates. MOFs usually have high porosity and specific surface areas that make them adequate candidates for catalytic applications both as high-surface-area supports and as intrinsic catalysts.[26,27] MOFs have been used as catalysts for various types of oxidation reactions in the liquid phase, for example, alcohol oxidation,[28] epoxidation,[29–32] hydrocarbon oxidation,[33–36] hydroquinone oxidation,[37] the oxidation of organic sulfides,[38] and the oxidation of aromatics.[39] For these oxidation reactions especially, a certain degree of deactivation is frequently observed. Co-based MOFs have been used previously for the oxidation of cyclohexene with *t*BuOOH, resulting mainly in allylic oxidation products.[40,41]

In this study, the epoxidation of styrene and stilbene by molecular oxygen is investigated by using DMF as the solvent and the MOF catalyst STA-12(Co). The MOF structure has been resolved by Rietveld refinement and it features an analogous structure to STA-12(Ni)[42] and is therefore a high-metal-containing alternative to the frequently used zeolites. The influence of important reaction parameters is examined in detail to clarify the role of the Co–MOF. Furthermore, the role of various activating and deactivating additives on the catalytic reaction was investigated. In situ electron paramagnetic resonance (EPR) and X-ray absorption spectroscopy (XAS) studies provided additional valuable mechanistic information.

Results

Synthesis and characterization of STA-12(Co): Powders obtained from the reaction of cobalt(II) acetate with H_4L ($L = C_6H_{12}N_2P_2O_6$) were characterized by powder X-ray diffraction and were found, as previously reported,[43] to have a similar characteristic diffraction pattern to that observed for STA-12(Ni)[42] (see the Supporting Information). Optimization of the reaction conditions indicated that a cobalt acetate to H_4L ratio of 2:1 at a starting pH of 8 yields phase-pure samples of STA-12(Co). Powder diffraction data were analyzed by Le Bail fitting by using the routines within the GSAS suite of programs[44] and with the unit cell of as-prepared STA-12(Ni)[42] as the starting point. Refinement of the unit-cell parameters indicated that as-prepared STA-12(Co) crystallized in the same rhombohedral space group as STA-12(Ni), but with a slightly larger unit cell (space group: $R\bar{3}$; hexagonal setting: $a = 28.0942(19)$, $c = 6.2846(3)$ Å).

Thermogravimetric analysis (TGA) in air, with a ramp rate of 1.5 °C min^{-1} up to 900 °C, showed two weight-loss events (see the Supporting Information). The first weight loss of 18.3 wt % (20–85 °C) was assigned to the removal of physisorbed water from the pores. This was immediately followed by an increase in gradient of the TGA plot, marking a second weight loss of 6.8 wt % (85–108 °C), assigned to the loss of chemisorbed water from the Co^{2+} ions. Between 108 °C and 270 °C, there were no significant weight losses on heating, indicating that the dehydrated material is thermally stable up to this temperature.[45] Above 270 °C, further weight losses are observed that are thought to be due to structural collapse.

Powder X-ray diffraction data for a sample of STA-12(Co) dehydrated under vacuum at 150 °C show that the material undergoes a structural transition on dehydration, which is reversible on subsequent rehydration of the material (see the Supporting Information). Energy dispersive X-ray (EDX) spectroscopy indicated a Co/P ratio of 1:1 (see the Supporting Information) and, in combination with the TGA data, a composition for STA-12(Co) of $Co_2(H_2O)_2L{\cdot}5H_2O$, in which $L = C_6H_{12}N_2P_2O_6$, was postulated. This hypothetical composition shows reasonable agreement with the obtained elemental analysis data (calculated (%): C 14.0, N 5.5; found: C 14.53, N 4.95).

The structure of STA-12(Co) was refined by the Rietveld method, by using the GSAS suite of programs,[44] against laboratory powder X-ray diffraction data ($Fe_{K\alpha 1}$, $\lambda = 1.930642$ Å). The structure of as-prepared STA-12(Ni) was used as the starting model, with the unit cell derived from Le Bail fitting. Positions of physisorbed water molecules were retained from STA-12(Ni) and the reduced number of physisorbed water was accounted for by changes in the occupancy of the water sites. Full details of the refinement are given in the Supporting Information (the refined structure is shown in Figure 1). The final profile fit (Figure 2) shows good agreement with the observed diffraction pattern, with a final $R_{wp} = 3.51$ %, indicating that STA-12(Co) is isostructural with STA-12(Ni).

The porosity of STA-12(Co) was confirmed by N_2 adsorption at 77 K on dehydrated samples of STA-12(Co). Samples were pretreated at 140 °C for 180 min and found to have a pore volume of 0.10 cm^3 g^{-1} (at $p/p_0 = 0.4$; Figure 3). The porosity of STA-12(Co) is approximately half that of STA-12(Ni). Both the uptake of gas from $p/p_0 > 0.5$ and the hysteresis are caused by intercrystalline void space, that is, there are void spaces between the agglomerated crystallites which have approximately mesoporous free diameters, giving rise to similar isothermal characteristics to materials containing mesopores.

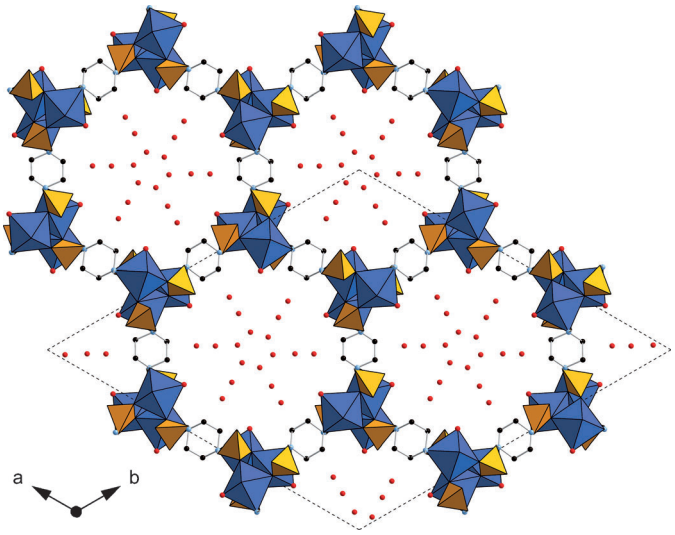

Figure 1. Refined structure of hydrated STA-12(Co), showing one complete unit cell and the hexagonal arrangement of the channels. Positions of the physisorbed water molecules are shown as O atoms (red spheres) within the unidirectional channels. Dashed lines indicate one unit cell.

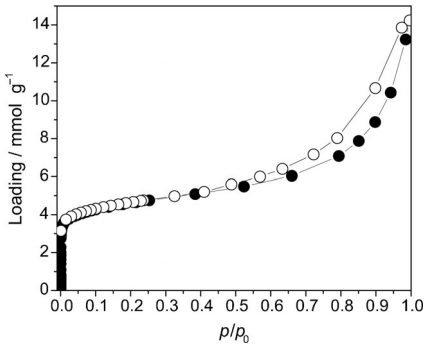

Figure 3. Isotherm for the adsorption (●) and desorption (○) of N_2 on fully dehydrated STA-12(Co) at 77 K, showing an uptake of 2.9 mmol g^{-1} ($p/p_0 = 0.4$), and indicating that STA-12(Co) has a pore volume of 0.10 cm^3 g^{-1}. STA-12(Co) was pretreated by heating at 140 °C for 180 min under vacuum.

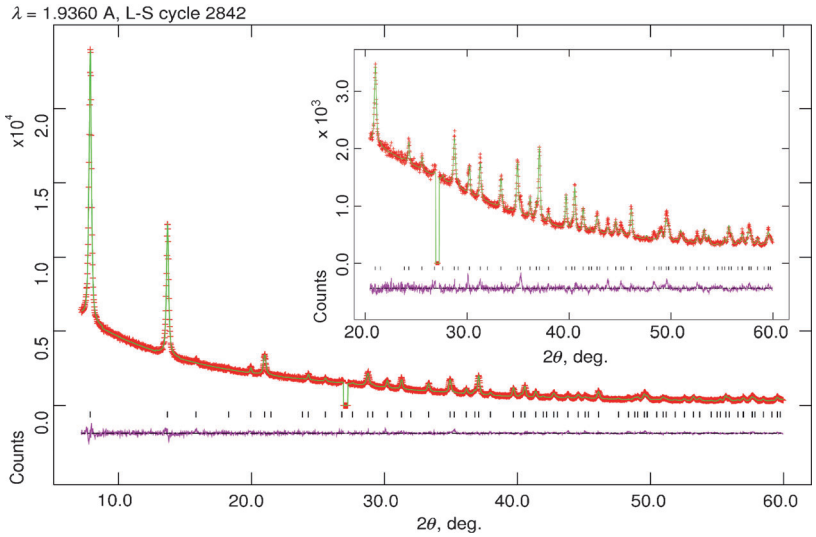

Figure 2. Rietveld plots in the range $2\theta = 7.2$–60° and 20–60° (inset) for the refinement of STA-12(Co) from laboratory powder diffraction data (Stoe STADI P, $Fe_{K\alpha 1}$, $\lambda = 1.936042$ Å) measured at 298 K. Experimental data: red; fitted data: green; difference plot: purple; peak positions: black ticks. Peak at $2\theta = 27$° excluded, shown as vertical green lines in the fitted data.

STA-12(Co) as a heterogeneous epoxidation catalyst in DMF: The Co-based metal–organic framework was used as an epoxidation catalyst in DMF with molecular oxygen as the oxidant. In the first set of experiments, the epoxidation of styrene was investigated, giving styrene oxide, benzaldehyde, and benzoic acid as the major products detectable by GC and accounting for roughly 60% of the mass balance. The rate of product formation increased steadily in the beginning of the reaction, giving a noticeable induction period of approximately 30 min (Figure 4). The reaction was complete after 5 h and exhibited only a very low selectivity (21%) to styrene oxide. Roughly twice the amount of *N*-formyl-*N*-methylformamide (FMF) was formed during the reaction with respect to converted styrene. The incomplete mass balance obtained from GC analysis throughout the reaction might be accounted for by styrene oligomerization. Thus, (*E*)-stilbene was used for further studies as it is less prone to oligomerization.

(*E*)-Stilbene was readily converted into *trans*-stilbene oxide and the mass balance from GC analysis was close to 100% (Figure 5). Almost full conversion was obtained after 12 h and the amount of FMF was found to be about 1.6 times the quantity of converted stilbene. It should be noted that the formation of a slightly larger amount of FMF in the case of styrene epoxidation took only 5 h. It appears that FMF formation depends on the type of olefin and correlates with the conversion. FMF was also formed in the absence of a substrate but in significantly lower quantities. The selectivity for *trans*-stilbene oxide was close to 90% and a low selectivity toward benzaldehyde (≈5%) was found, assuming that two molecules of benzaldehyde are formed from one (*E*)-stilbene molecule. Co_3O_4 also exhibited some catalytic activity (Table 1), whereas essentially no product formation was found in the absence of a catalyst. An analogous mixed metal STA-12(Co,Ni) catalyst (1:3 ratio) showed virtually no catalytic activity (3% conversion after 12 h), suggesting that the organic backbone of the MOF is inactive. In comparison to the (*E*)-isomer, (*Z*)-stilbene was epoxidized very slowly,

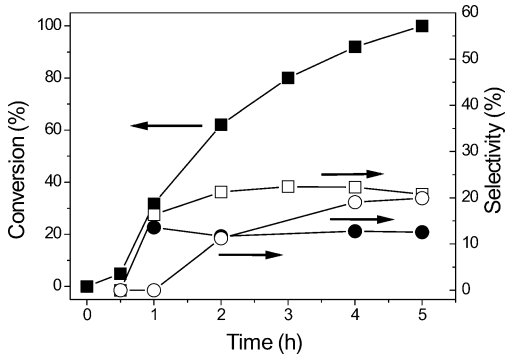

Figure 4. The epoxidation reaction of styrene with the Co-based metal–organic framework material STA-12(Co). The graph shows styrene conversion (■), as well as the selectivity for styrene oxide (□), benzaldehyde (●), and benzoic acid (○). Reaction conditions: styrene (2.0 mmol), biphenyl (100 mg), DMF (30 mL), O_2 (50 mL min^{-1}), and STA-12(Co) (2.0 mg) at 100 °C.

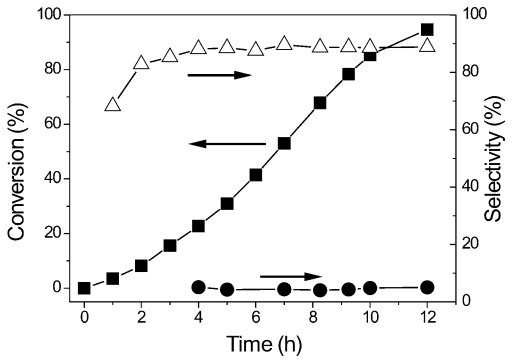

Figure 5. The epoxidation reaction of (*E*)-stilbene by use of STA-12(Co). The graph shows (*E*)-stilbene conversion (■), as well as the selectivity for *trans*-stilbene oxide (Δ) and benzaldehyde (●). Reaction conditions: (*E*)-stilbene (2.0 mmol), biphenyl (100 mg), DMF (30 mL), O_2 (50 mL min^{-1}), and STA-12(Co) (2.0 mg) at 100 °C.

Table 1. Aerobic epoxidation of (*E*)-stilbene in DMF.[a]

Catalyst	Time [h]	Conversion [%]	Selectivity [%]
–	10	<1	–
Co_3O_4	12	15	68
STA-12(Co)	12	95	89
STA-12(Co, Ni) (Co/Ni = 1:3)	12	3	60

[a] Reaction conditions: (*E*)-stilbene (2.0 mmol), Co (0.4 mg), biphenyl (100 mg), DMF (30 mL), and O_2 (50 mL min^{-1}).

although it also gave *trans*-stilbene oxide (see Table 3, entry 1 below). Isomerization of (*Z*)- to (*E*)-stilbene was not observed.

To assess its stability, the catalyst was tested for reusability. Some deactivation was observed that mainly caused a longer induction period, after which time the reaction rates were comparable (see the Supporting Information). SEM and XRD analysis of a fresh and a used sample of the catalyst did not show any significant differences, suggesting that the MOF remained in its initial crystalline state (Figure 6).

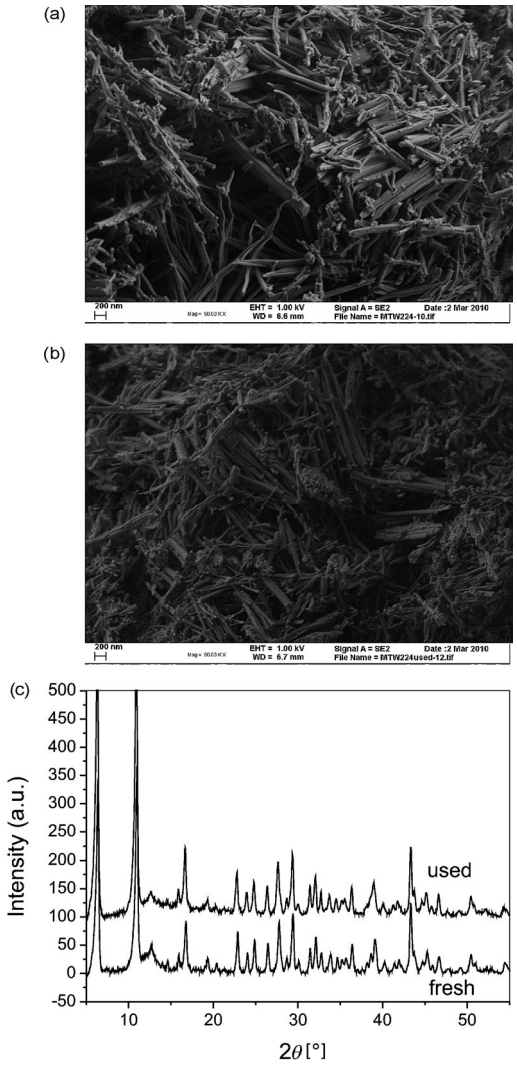

Figure 6. Comparison of fresh and used STA-12(Co) catalyst. a) SEM image of the fresh catalyst (scale bar: 200 nm), b) SEM image of the used catalyst (scale bar: 200 nm), and c) XRD pattern of fresh and used catalysts.

One reason for the observed deactivation might be the blocking of pore entrances or poisoning of free Co sites by amines formed from DMF during the reaction (see below).

Heterogeneous versus homogeneous catalysis: An important issue in MOF catalysis is to assess whether the catalysis proceeds mainly homogeneously or heterogeneously[26,46] since dissolvable impurities or MOF degradation might also account for any observed catalytic activities. Thus, the catalyst was removed by hot filtration after the induction period. As can be seen in Figure 7, the reaction proceeds after catalyst removal, but with a significantly reduced reaction rate.

Indeed, analysis of the reaction mixture by atomic adsorption spectroscopy (AAS) showed some Co leaching of 0.40 ppm, amounting to approximately 3% of the employed Co. Subsequent dissipation of the MOF during the reaction can, however, be excluded as a cause for the catalytic activi-

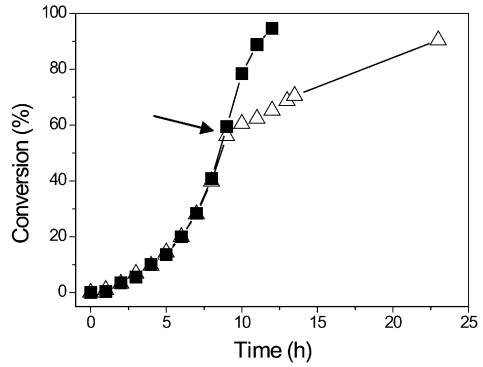

Figure 7. Comparison of the epoxidation with and without catalyst removal (after 9 h as indicated by the arrow). (■) (*E*)-stilbene conversion with STA-12(Co); (Δ) (*E*)-stilbene conversion with STA-12(Co) removal after 9 h. Reaction conditions: (*E*)-stilbene (4.0 mmol), biphenyl (100 mg), DMF (30 mL), O_2 (50 mL min^{-1}), and STA-12(Co) (2.0 mg) at 100 °C.

ty and the induction period; addition of (*E*)-stilbene to an oxygen-pretreated mixture of the Co–MOF and DMF (100 °C over 12 h) did not result in a higher reaction rate. In fact, the induction took even longer due to catalyst deactivation and a similar amount of leaching was found (0.44 ppm). Overall, this indicates that the main catalytic route is heterogeneous in nature although a minor contribution from homogeneous catalysis cannot be excluded.

Indeed, homogeneously dissolved Co salts (cobalt(III) acetylacetonate and cobalt(II) acetate) show considerable activity. By using the same amount of Co as in the heterogeneous experiments, both (*E*)- and (*Z*)-stilbene were converted faster (Figure 8) and without exhibiting an induction period. The conversion of (*E*)-stilbene occurred in two kinetically distinct phases; in the first phase, the reaction was (pseudo-)zeroth-order with respect to the substrate concentration. Toward the end of the reaction the amount of substrate became rate limiting and so the reaction became (pseudo-)first order. In contrast, the conversion of (*Z*)-stilbene always proceeded as a (pseudo-)first-order reaction (after the short initial induction period). The selectivities were similar to those with the MOF catalyst and in the vicinity of 90% for (*E*)- and 80% for (*Z*)-stilbene. Interestingly, both Co^{II} (from $Co(ac)_2{\cdot}4H_2O$; ac = acetyl) and Co^{III} (from $[Co(acac)_3]$; acac = acetylacetonate) salts were equally active at the same concentration, meaning that the Co oxidation/reduction occurs rapidly and is not a limiting factor for the homogeneous catalyst. The difference in induction time between homogeneous and heterogeneous catalysts apparently does not result from pore-diffusion limitations (due to the extensive microporous system) since a simple initial inhibition because of slow stilbene diffusion into the micropores of the MOF can be ruled out as a reason; keeping the MOF catalyst and (*E*)-stilbene in DMF under a high N_2 flow for 12 h and then switching to oxygen did not reduce the induction period.

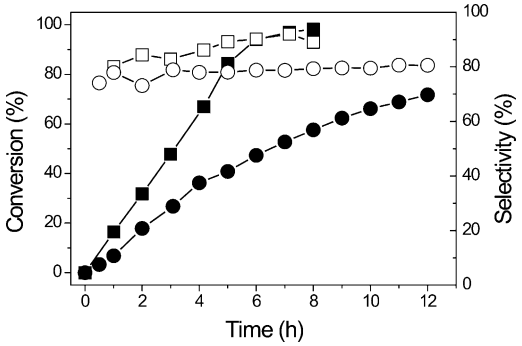

Figure 8. Comparison of the epoxidation reaction of (*E*)- (■,□) and (*Z*)-stilbene (●,○) with homogeneous cobalt complexes. The graph shows (*E*)-stilbene conversion (■) and the selectivity for the formation of *trans*-stilbene oxide (□) from (*E*)-stilbene, as well as (*Z*)-stilbene conversion (●) and the selectivity for the formation of *trans*-stilbene oxide (○) from (*Z*)-stilbene. Reaction conditions: stilbene (2.0 mmol), biphenyl (100 mg), DMF (30 mL), O_2 (50 mL min^{-1}), and $[Co(acac)_3]$ (2.4 mg).

Influence of reaction parameters: As the next step, the effects of temperature, catalyst amount, substrate concentration, and oxygen flow rate were studied. Higher temperatures enhanced the reaction rate. At 60 °C, the conversion was only 7% after 10 h, whereas at 120 °C the reaction was almost complete (95% conversion, Figure 9a). Interestingly, the selectivity for the epoxide was lowest at 60 °C (48%). Low epoxide selectivity was, on the other hand, always obtained at low conversions. Above 80 °C, the temperature had little effect on the epoxide selectivity, which was then close to 90%.

The reaction rate was highly dependent on the oxygen flow rate (Figure 9b). This is interesting because the overall reaction rate is low and the consumption of oxygen should be overcompensated for by low gas flow rates. Epoxidations with gold catalysts proceed at similar rates[6] and were conducted in an open reaction vessel without any additional oxygen flow. In this study, the faster removal of volatile catalyst poisons, such as amines (see below), might be the cause of the benefits from high gas flow rates. Consequently, reaction mixtures became considerably darker after 12 h when the flow rate was low, potentially due to amine oxidation products. This was, however, not the sole reason for the observed effect. The use of air instead of pure oxygen with the same flow rate resulted in lower conversions. After 6 h, the conversion was 8% with an air flow of 50 mL min^{-1} compared with 38% with 50 mL min^{-1} oxygen. Thus, high oxygen availability is crucial to this reaction.

The reaction rate did not increase steadily with the amount of catalyst (Figure 9c), but rather exhibited an optimal cobalt to substrate ratio of 0.34 mol% (80% conversion after 10 h) and larger quantities of cobalt did not significantly influence conversion under the chosen conditions, as has been found previously.[17] This might indicate that the reaction rate is limited by mass transfer effects.

Furthermore, the substrate concentration had a peculiar effect on the catalytic process (Figure 9d). With a higher initial concentration of reactants, a higher conversion was found after 10 h when keeping the catalyst/substrate ratio

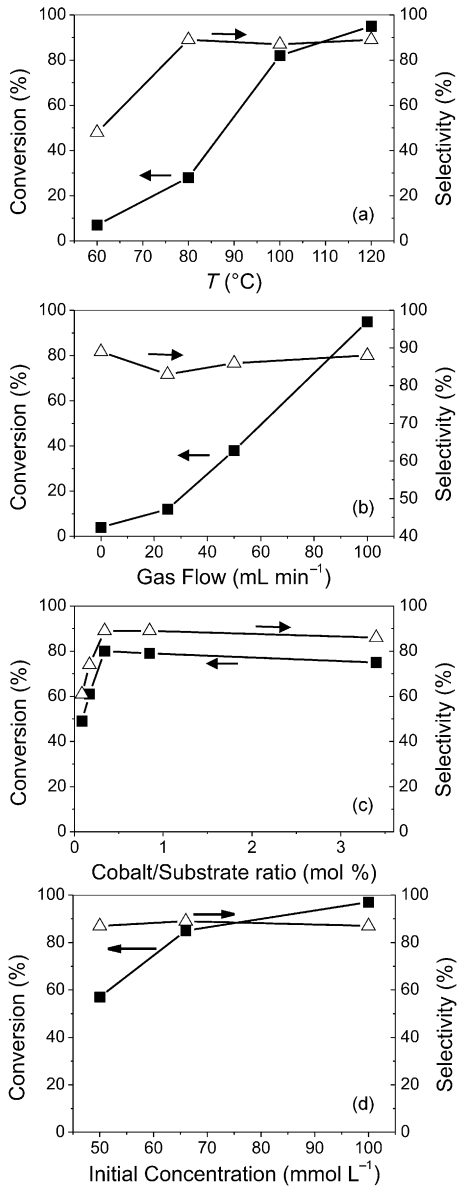

Figure 9. The influence of a) temperature, b) oxygen flow, c) catalyst amount, and d) reactant concentration on the epoxidation of (*E*)-stilbene. Reaction conditions: (*E*)-stilbene (2.0 mmol), biphenyl (100 mg), DMF (30 mL), O_2 (50 mL min^{-1}), STA-12(Co) (2.0 mg) at 100 °C for 10 h. Variations: a) temperature: 60–120 °C; b) oxygen flow: 0–100 mL min^{-1} for 6 h; c) substrate to catalyst ratio: 30–1200; d) DMF: 20–40 mL (■ = (*E*)-stilbene conversion; Δ = epoxide selectivity).

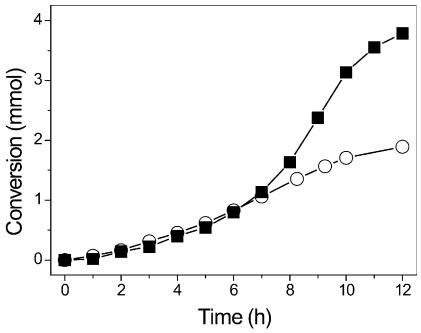

Figure 10. Conversion (in mmol) versus time profile at different substrate/catalyst ratios. Reaction conditions: (*E*)-stilbene (2.0 (○) and 4.0 mmol (■)), biphenyl (100 mg), DMF (30 mL), O_2 (50 mL min^{-1}), and STA-12(Co) (2 mg) at 100 °C.

constant, that is, by using different amounts of solvent. In this way, the solvent-to-catalyst ratio also changes. This effect was, however, only seen for long reaction times and variations in the concentration through the solvent amount. When varying the amount of substrate, but leaving the catalyst and solvent amount the same (Figure 10), the reaction rate (expressed in moles/time) was barely sensitive to the substrate concentration at sufficiently high concentrations, as was also observed with the homogeneous Co catalyst (see above). Thus, the heterogeneous reaction rate is initially not dependent on the substrate concentration, and at the same time steadily increasing.

The choice of solvent played a vital role. The use of toluene as the solvent did not yield any epoxidation products whereas mixtures of toluene and DMF permitted some catalytic activity. *N*,*N*-Dimethylacetamide (DMAc), another amide solvent, also proved to be a suitable solvent, affording an even higher reaction rate (compare Table 2, entries 1 and 2). With similar conditions to those used previously, full conversion (97%) was achieved after only 8.5 h compared with 12 h in DMF. On the other hand, the selectivity for *trans*-stilbene oxide was markedly lower, that is, around 60% compared with approximately 90% in DMF. The generally higher selectivity for benzaldehyde in DMAc might explain the higher reactivity in this solvent (see below). No reaction was observed for pure (*E*)-stilbene at 130 °C in contrast to a Co^{II}-exchanged heteropoly acid catalyst tested in the oxidation of styrene to form benzaldehyde.[47] Likewise, no reaction was observed in a 1:1 mixture of DMF and water, making the latter an inhibitor in high concentrations.

Amines as inhibitors: In a closed reaction system (that is, an autoclave), the selectivity and conversion dropped significantly even though relatively high oxygen pressures were applied (Table 2, entry 3) resulting in high oxygen availability, which had proved to be beneficial in experiments performed in an open reactor. Reference [23] also states a

Table 2. Influence of solvent, closed/open system, and additives on the epoxidation reaction.[a]

Entry	Solvent	O_2 flow[b]/ pressure[c]	Additive	Time [h]	Conversion [%]	Selectivity [%]
1	DMF	50 mL min^{-1}	–	12	95	89
2	DMAc	50 mL min^{-1}	–	8.5	97	64
3	DMF	7.5 bar	–	10	25	52
4	DMAc	7.5 bar	–	10	73	41
5	DMF	7.5 bar	NaH_2PO_4	10	6	64
6	DMF	7.5 bar	CH_3COOH	10	49	68

[a] Reaction conditions: (*E*)-stilbene (2.0 mmol), STA-12(Co) (2.0 mg), biphenyl (100 mg), and DMF (30 mL) at the oxygen flow/pressure indicated. [b] Flowing oxygen in an open glass reactor system. [c] Oxygen pressure applied in a closed reactor system.

lower conversion observed in closed reactors although other studies investigating epoxidation reactions in a closed reactor under elevated oxygen pressure only found small differences. [17] One reason for the higher conversion in open-reactor systems might be the formation of amines from DMF decomposition, which coordinate at the free Co sites. The high volatility of the amines ensures their quick removal in an open reactor, which is not possible in an autoclave. Additionally, in a closed system, epoxidation in DMAc gave a significantly higher conversion (Table 2, entry 4) than in DMF. DMAc is more stable toward decomposition[48] and thus the amine concentration should be lower in this solvent. This also explains, at least in part, the lower observed catalytic activity in DMF compared to DMAc in an open system. Although the addition of NaH_2PO_4 as an amine scavenger had a negative effect on the epoxidation reaction (Table 2, entry 5), the presence of acetic acid (Table 2, entry 6) doubled the conversion. In an open system, both the activity of the MOF catalyst and of dissolved Co species could be completely inactivated by constant addition of diethylamine. This underlines the fact that a free coordination site at the Co centers is required for catalytic activity.

Involvement of radical species: DMF promoted epoxidations are widely assumed to occur through a radical reaction pathway. Indeed, the reaction rate was significantly decreased upon addition of either of two different radical scavengers, that is, 4-*tert*-butylcatechol and 2,6-di-*tert*-butyl-4-methylphenol. Radical reactions usually feature an induction period—as observed in this study—in order to form a steady-state radical concentration. However, the addition of radical initiators, such as azobis(isobutyronitrile) (AiBN), had no effect on the initial reaction rate. The initial conversion was fast with *tert*-butylhydroperoxide (TBHP; 5 mol%) but then continued as in the other experiments. TBHP can thus be regarded as an epoxidizing reagent that is rapidly consumed in the beginning of the reaction and not as an initiator.

To further shed light on the possible involvement of radicals in this reaction, the reaction mixture was investigated with EPR spectroscopy under in situ conditions. However, free organic radicals could not be detected although potential free radicals could be EPR inactive due to coupling or their concentration could be below the limit of detection. The inhibiting effect of radical scavengers might also be due to adsorption or coordination to free Co sites.[49] A signal at $g=2.0076$ was found that can be ascribed to Co^{III}–O_2^{*-} (superoxo) species formed from the reaction of Co^{II} with oxygen.[50] These can already be found in the solid catalyst measured ex situ and thus are not formed specifically under the reaction conditions. Hence, their formation is likely not connected to the induction period. Note that Co^{III}-peroxo species, which might also form from reaction of Co^{II} with O_2, are not EPR active.[51]

Co-epoxidation of styrene and (*E*)-stilbene: Driven by the observation that styrene epoxidation not only proceeds faster but also features a shorter induction period, the co-epoxidation of styrene and (*E*)-stilbene was investigated, thus doubling the substrate/catalyst ratio (Figure 11a). Al-

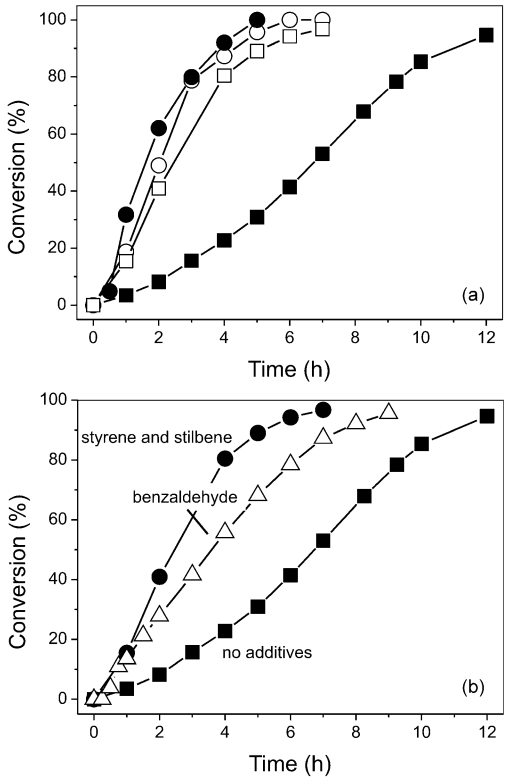

Figure 11. Co-epoxidation of styrene and (*E*)-stilbene and the effect of the presence of benzaldehyde on the reaction. a) Comparison of separate styrene and (*E*)-stilbene conversion (■ = (*E*)-stilbene, ● = styrene) with the co-epoxidation of styrene (○) and (*E*)-stilbene (□). b) The effect of benzaldehyde addition (0.2 mmol) on (*E*)-stilbene conversion (● = styrene and stilbene; △ = benzaldehyde; ■ = no additives). Reactions conditions: (*E*)-stilbene and/or styrene (2.0 mmol), biphenyl (100 mg), DMF (30 mL), O_2 (50 mL min^{-1}), and STA-12(Co) (2.0 mg) at 100 °C.

though the catalyst amount was not increased, the presence of styrene induced much faster conversion of (*E*)-stilbene. At the same time, the conversion of styrene became only slightly slower at medium conversions. Co-epoxidation with styrene also had a strong effect on the conversion of (*Z*)-stilbene, which increased from 11 to 58% after 10 h. This effect was not observed for the homogeneous Co catalysts for either (*E*)- or (*Z*)-stilbene epoxidation (Table 3, entries 3 and 4) and might be an effect related to the special features of the MOF. Styrene, being smaller than (*E*)-stilbene, can diffuse more easily into the micropores of the MOF. However, a transfer-epoxidation from styrene oxide to (*E*)-stilbene does not account for the styrene promotion because styrene oxide as an additive did not have any promoting effect. even in large quantities. Oxygen transfer from styrene oxide as the potential oxidizing agent of (*E*)-stilbene was also not observed under reaction conditions with a N_2 flow instead of O_2.

Table 3. Epoxidation of (*Z*)-stilbene with heterogeneous and homogeneous Co catalysts.[a]

Entry	Catalyst	Styrene promotion	Conversion [%]	Selectivity [%]
1	STA-12(Co)	no	11	92
2	STA-12(Co)	yes	58	86
3	$[Co(acac)_3]$	no	66	80
4	$[Co(acac)_3]$	yes	65	92
5	Co_3O_4	no	9.4	53

[a] Reaction conditions: (*Z*)-stilbene (2.0 mmol), Co (6.8 μmol) as the catalyst, biphenyl (100 mg), and DMF (30 mL) for 10 h with flowing O_2 (50 mL min^{-1}). Optional styrene addition: 2.0 mmol.

Two major differences between MOF-catalyzed styrene and (*E*)-stilbene conversion are the higher reaction rate for the reaction of styrene and the higher selectivity for benzaldehyde formation (styrene: ca. 12%; (*E*)-stilbene: ca. 5%) for the former. Thus, styrene conversion affords a comparably high benzaldehyde concentration even at the beginning of the reaction. Indeed, benzaldehyde being the major byproduct could explain the observed promoting effect—as with the presence of styrene, the (*E*)-stilbene reaction rate was enhanced by addition of substoichiometric amounts of benzaldehyde (Figure 11b). Nevertheless, benzaldehyde did not have a promoting effect on the activity of homogeneous Co catalysts.

Formation of oxidizing species: Triphenylphosphine is frequently used to scavenge thermally unstable peroxides for GC analysis. Furthermore, in this study, triphenylphosphine oxide was found when PPh_3 was added to the samples taken for GC analysis, indicating the presence of peroxides. Over time, the amount of peroxide increased steadily. In a similar manner to FMF formation, peroxides were also formed in lower amounts in the absence of the substrate. With homogeneous catalysts, the formation of peroxides proceeded at a higher rate that correlates with the higher product-formation rate. In general, peroxides can serve as epoxidizing agents, as shown, for example, for gold catalysts.[9,52] In this case, however, peroxides proved to be almost irrelevant for the epoxidation, since an oxygen pretreated (that is, peroxide-containing) mixture of DMF and Co–MOF did not affect the (*E*)-stilbene epoxidation after substrate addition under a N_2 atmosphere; after 12 h, a conversion of only 3% was found with a low epoxide selectivity of 60%, representing only a minor reaction pathway. This is principally in accordance with the lower epoxidation activity of H_2O_2 in DMF with respect to O_2 described previously.[16,19] Furthermore, in this study, the addition of PPh_3 to the reaction mixture inhibited the formation of products and only small amounts of $OPPh_3$ were formed. PPh_3 likely coordinates to the free Co sites and thus acts as a catalyst poison.

EXAFS investigations under reaction conditions: To understand the complex catalytic process more thoroughly, XAS experiments were conducted. The Co K-edge FT EXAFS spectra of the fresh and used catalyst were very similar. Fit results suggest that the structure of STA-12(Co) is similar to that of hydrated STA-12(Ni)[42] with a Co–O/N coordination number of 6 and an additional Co···Co and Co···P shell (Table 4). It should be noted that during fitting no distinction between Co–N and Co–O contributions was made. The large Debye–Waller factor indicates a low symmetry of the Co–N/O polyhedra. In addition, the similar lengths of the Co···Co and Co···P backscattering paths complicate their differentiation and lead to inaccurate coordination numbers. The fitted Co···Co and Co···P distances are in reasonable agreement with XRD data.

Table 4. Fit results for fresh (ex situ) and used (ex situ) STA-12(Co), as well as STA-12(Co) under the reaction conditions (in situ). The damping factor S_o^2 was set to 0.8 in all fits.

Shell	*N*	*R* [Å]	σ^2	ΔE_0 [eV]
fresh STA-12(Co)[a]				
Co–O	5.9	2.10	0.0085	−3.1
Co···Co	4.1	3.23	0.0049	−3.1
Co···P	4.7	3.23	0.0032	−3.1
used STA-12(Co)[b]				
Co–O	5.4	2.09	0.0077	−4.1
Co···Co	1.1	3.23	0.0023	−4.1
Co···P	4.4	3.28	0.010	−4.1
STA-12(Co) in DMF (in situ)[c]				
Co–O	2.5	2.04	0.0077	−5.2
Co···Co	2.0[d]	3.18	0.0097	−5.2
Co···P	3.3	3.20	0.013	−5.2

[a] Fitted in $k = 2.5$–13 Å^{-1}; $R = 1.2$–3.8 Å; residual 5.1. [b] Fitted in $k = 2.5$–13 Å^{-1}; $R = 1.2$–3.6 Å; residual 7.7. [c] Fitted in $k = 2.5$–12 Å^{-1}; $R = 1.2$–3.2 Å; residual 3.9. [d] Fixed during refinement.

The catalyst was also investigated in situ with X-ray absorption spectroscopic measurements in a closed autoclave (for safety reasons). Upon addition of DMF to the catalyst pellet, the white-line intensity dropped and the pre-edge peak became more pronounced (Figure 12b). The latter is usually ascribed to a reduction in symmetry that might be caused by incorporation of DMF into the pores of the catalyst. Heating the catalyst and the reaction mixture to 100°C did not induce further structural changes in the catalyst over 8 h, which therefore showed no major catalyst decomposition. The data quality was too poor for individual data fitting of each spectrum but required averaging of all of the similar spectra in DMF (Table 4). It appears that the fitted Co···O/N coordination number decreases significantly on addition of solvent due to a change in the geometry of the Co coordination sphere as is also suggested by the pre-edge feature. It should be noted, however, that EXAFS is not a surface-sensitive method and thus changes occurring at the outer surface of the MOF are most likely not observable.

Discussion

The presented STA-12(Co) catalyst effectively catalyzes the epoxidation of olefins in DMF. The absolute amount of catalyst necessary for a reasonable conversion could be de-

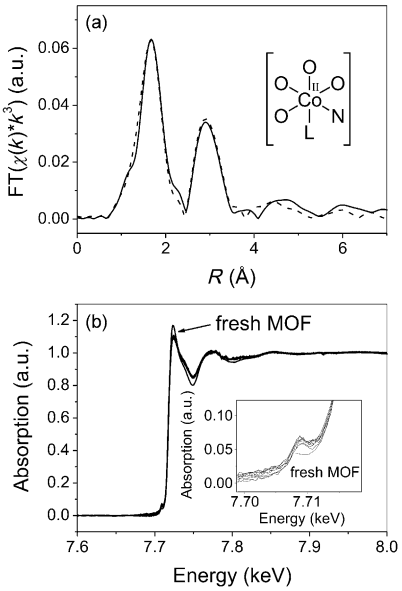

Figure 12. EXAFS and XANES investigations of the as-prepared and in use/used STA-12(Co). a) Fourier transformed Co K-edge EXAFS data of the fresh (– – –) and used (——) catalyst; b) in situ Co K-edge XANES spectra of STA-12(Co) before and during the epoxidation in DMF; inset: the pre-edge region.

creased by two orders of magnitude compared with reports in the literature on zeolite catalysts.[21] It should be noted that the high metal content in comparison with zeolites is most likely not the origin of the higher activity (with respect to the catalyst mass); this selectivity difference is more likely due to an intrinsically higher activity of the active sites. The conversion of styrene occurred quickly, but with only very low selectivity (around 20%) and was accompanied by the formation of unknown (presumably oligomeric) side products, as suggested by the incomplete mass balance. This is likely a common side reaction for styrene in DMF at elevated temperatures.

Various examples in the literature of aerobic epoxidations in DMF with Co-based solid catalysts (for examples see, references [22,53]) report styrene oxide selectivities of higher than 60%, which are, however, calculated on the basis of benzaldehyde and styrene oxide being the only products. The use of the same estimation matrix for this study would also result in selectivities well above 60%. Additionally, styrene was distilled prior to its use in this study so that stabilizers were removed. In contrast, the MOF catalyst converted (*E*)-stilbene with high selectivity, between 80 and 90%. Average turn-over frequencies were higher in this study, at around 20 h^{-1}, compared with maxima around 8 h^{-1} given in Reference [21] under similar conditions calculated on the basis of the overall Co amount. Alongside the epoxidation reaction, large amounts of byproducts not directly attributable to the olefin were formed in over- and near-stoichiometric amounts, that is, *N*-formyl-*N*-methylformamide (FMF) as a solvent oxidation product and presumably free peroxides, both hinting at the complexity of the reaction mechanism.

A side-by-side comparison of the MOF catalyst with the homogeneous catalysts employed here is difficult due to the difference in ligand spheres. Better homogeneous analogues of the MOF would bear an *N*,*N*′-piperazinebis(methylenephosphonate) ligand but due to the distinct Co network in the MOF this would still not allow for accurate comparison. Differences show, however, that effects seen for the MOF cannot be generalized for all types of Co catalyst (for example, the homogeneous catalysts behave differently). A major difference is the appearance of an induction period with the MOF. One reason for the induction period was traced back to the gradual formation of benzaldehyde, which was found to be connected to the catalytic activity of the MOF and served as an explanation for the unexpected promoting role of another substrate, styrene, on the conversion of the investigated stilbene isomers.

Other reasons for the induction period were also investigated. For example, it seems unlikely that pore diffusion had an effect despite the fact that the micropores of the MOF (ca. 1 nm) are similar in size to the stilbene isomers (ca. 1 nm) and therefore diffusion should influence the induction period (and reaction rate)—if epoxidation takes place in the pores. Since the presence of benzaldehyde will hardly influence stilbene diffusion and MOF pretreatment with stilbene under N_2 did not shorten the induction period, the MOF is likely active through only its outer surface. The efficacy of the MOF catalyst is therefore still limited by diffusion issues relating to the inaccessibility of the MOF micropores. Consequently, smaller particle sizes (for example, in a supported version of the MOF) could allow a further reduction of the overall amount of catalyst required.

Opre et al.[23] have suggested that epoxidation might occur via a DMF-derived peroxide that would need to be formed prior to product formation. Although DMF oxidation is the cause of the pronounced solvent effect, a link between its conversion and the formed peroxides could not be established in this case. Subsequent leaching of the MOF to release catalytically active Co species is also not responsible for the initial increase in the reaction rate. The reaction was shown to be primarily heterogeneous and pretreatment of the MOF in DMF did not shorten the induction period although a small amount of leaching could be found.

Furthermore, in situ EPR investigations suggested that the formation of Co–O_2* species is also not the origin of the induction period because these are already present in fresh STA-12(Co). The formation of a steady-state radical concentration could also not be confirmed to be a cause for the induction period and the reaction. It should be noted that it is possible that the radical concentration was below the limit of detection by EPR spectroscopy. Thus, the primary reason for the induction period appears to be the formation of benzaldehyde, which then promotes the reaction.

The exact role of benzaldehyde in this reaction is unclear at this point, but its influence is not similar to the Mukaiyama epoxidation, because only tiny amounts of benzoic acid were detected and the mass balance was closed for the epoxidation of the stilbene isomers. Considering that radical

initiators had little effect on the reaction rate, benzaldehyde-derived radicals will likely also not be the origin of the observed activating effect. Since the presence of benzaldehyde affects the catalyst activity, this might serve as an explanation for the small influence of the amount of MOF used on the catalytic reaction, although mass transport limitations are also conceivable. Clearly, further studies are necessary to elucidate the effect of benzaldehyde.

With respect to the actual epoxidizing agent, three species are conceivable, from which free peroxides found in high concentrations can be excluded on the basis of the experimental results obtained in this study. The reaction of Co^{II} with O_2 can result in two different species, namely, Co-superoxo species and (mainly) binuclear Co-peroxo species.[52] These species are interrelated as $Co^{III}–O_2*$ can (possibly reversibly) bind to Co^{II} molecules with one available coordination site, as shown for Co complexes in water.[54–57] Binuclear Co-peroxo complexes also form in DMF.[58] In the cited studies, the formation of peroxo-species was favored over the formation of superoxo-species. Typical Co–Co distances in binuclear Co-peroxo complexes are around 4.5 Å,[58,59] which is similar to the Co–Co separation in the MOF (4.87 Å). However, the free coordination sites of the respective Co ions point toward the center of different channels, making the occurrence of binuclear peroxides unlikely because it would require significant restructuring of the MOF, which was not found by in situ EXAFS. Thus, radical superoxo species, found by EPR spectroscopy, appear to be reasonable candidates for explaining the epoxidation activity of the MOF material. It should be noted, however, that the chemical nature of surface-bound Co species is unknown and principally inaccessible by the characterization techniques employed herein.

With the assumption that Co superoxo species are required for catalytic activity, a preliminary mechanism is proposed, as shown in Scheme 1. The role of benzaldehyde in the MOF-catalyzed reaction was clearly observed and is interpreted in terms of an activation of the active site (step **1**) the exact nature of which still needs to be elucidated. Control of the catalyst activity by the benzaldehyde concentration would explain the limited influence of the MOF amount on the reaction rate (although mass transport limitations may also account for this observation). Activated Co^{II} sites then react with molecular oxygen, from which the formation of Co-superoxo radicals, which are sensitive to radical scavengers, is conceivable (step **2**). Competition for the free Co coordination site between the ligands present in the solution (for example, DMF and amines) and oxygen would explain the beneficial influence of high oxygen flow rates (step **2a**). In step **3**, the reaction between stilbene and Co-activated oxygen affords an intermediate complex. The formation of the epoxide is not concerted because both (*E*)- and (*Z*)-stilbene afford *trans*-stilbene oxide. Since the same product is formed from both stilbene isomers their difference in reactivity cannot be from desorption (step **4**), which is thus not the rate-limiting step. The remaining step requires regeneration of the catalyst from the Co^{III} species through oxidation of the solvent (step **5**), explaining both the strong solvent influence and the observed solvent oxidation. Regeneration of the catalyst would be fast compared with the other steps because the reaction rate clearly depends on the type of substrate. Although the proposed reaction mechanism is speculative, it explains the observations made in this paper. Nevertheless, more data is needed to provide evidence for the postulated intermediates.

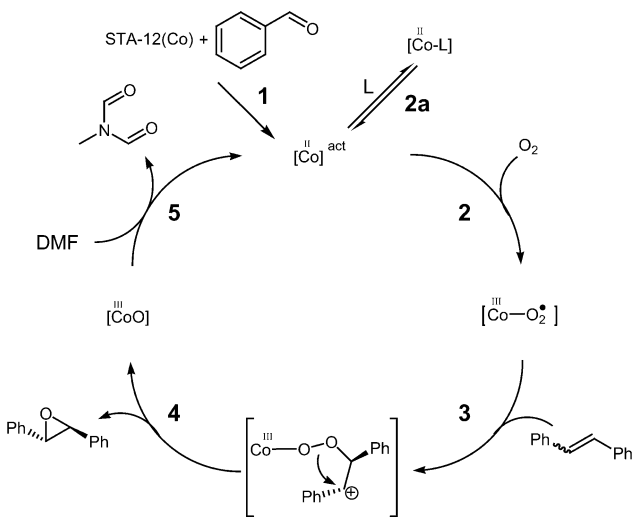

Scheme 1. Proposed reaction mechanism for the epoxidation of stilbene assuming an activated Co center as the active species.

Conclusion

The metal–organic framework STA-12(Co) features high activity in the aerobic epoxidation of various olefins in DMF. In comparison with the commonly applied zeolites, the absolute amount of catalyst was significantly reduced. The structure of STA-12(Co) is similar to the previously reported STA-12(Ni). The selectivity in styrene epoxidation was low due to substrate oligomerization. In contrast, both (*E*)- and (*Z*)-stilbene were epoxidized with high selectivities between 80 and 90%, featuring an induction period of a few hours. Within the catalytic reaction, the solvent served as a sacrificial reductant. Free peroxides formed in considerable amounts but could not be connected to the epoxidation reaction. The reaction rate increased with oxygen flow rate, higher temperatures, and substrate concentration (by varying solvent amounts). The substrate-to-catalyst ratio exhibited an optimum at approximately 0.3 mol% (with 50 mL min^{-1} O_2). The catalyst was reusable with only minor deactivation although no major structural changes were observed by SEM, XRD, and EXAFS spectroscopy, underlining the stability of the MOF under the reaction conditions. The reaction proceeded mainly heterogeneously, with minor contributions from leached Co. Homogeneous Co was indeed found to be very active for the epoxidation and exhibited no induction period. The substrate-dependent induc-

tion period of the Co-based MOF catalyst and the beneficial effect of styrene on stilbene epoxidation could be linked to the promoting effect of benzaldehyde, which is only observable for the Co–MOF catalyst and not for homogeneous Co catalysts. Both the reaction catalyzed by homogeneous Co and STA-12(Co) were (pseudo-)zeroth order with respect to the substrate at high concentrations. A feasible catalytic cycle accounting for the observations made in this study was proposed that should be further substantiated in future studies on other Co-based catalysts.

Experimental Section

Synthesis of STA-12(Co): STA-12(Co) was synthesized hydrothermally by reaction of cobalt(II) acetate and *N*,*N*′-piperazinebis(methylenephosphonic acid) (H_4L), prepared by the method reported by Mowat et al.[60] In a typical synthesis cobalt(II) acetate tetrahydrate (Sigma), H_4L, potassium hydroxide solution (freshly prepared, 1 mol L^{-1}), and water (20 mL) were mixed, to give a reaction ratio of 2.0:1.0:2.12:900, in a Teflon lined autoclave (40 mL). The reaction was stirred for 30 min and an initial pH of 8 was recorded. The autoclave was then sealed and heated at 220 °C for 72 h. The resulting purple powder was collected by vacuum filtration, washed with water, and dried overnight at 40 °C. Phase purity was confirmed by powder X-ray diffraction using a Stoe STADI P powder diffractometer with an $Fe_{K\alpha1}$ radiation source ($\lambda = 1.930642$ Å). The composition of STA-12(Co) was determined jointly by elemental analysis by using a CEInstruments EA1110 CHNS analyzer, thermogravimetric analysis (TGA) by using a Netzsch TG 209, and energy dispersive X-ray spectroscopy (EDX) by using a JEOL JSM-5600 scattered-electron microscope (SEM) fitted with an Oxford Instruments INCA Energy 200 EDX system. Porosimetry measurements were made gravimetrically by using a Hiden Isochema IGA at 77 K.

Catalytic tests: Catalytic test reactions were performed in a three-necked flask (50 mL) equipped with a reflux condenser, magnetic stirrer, and gas inlet. Because the system was sensitive to minute amounts of Co, cleaning the flask with aqua regia prior to each experiment was necessary. In a typical reaction, the flask was charged with DMF (30 mL) and immersed in an oil bath kept at 100 °C under vigorous stirring. Oxygen was fed to the reaction mixture through the gas inlet at 50 mL min^{-1}. After a short time (15–30 min), biphenyl (100 mg) as an internal standard, STA-12(Co) (2.0 mg), and the olefin (2.00 mmol; styrene, (*E*)- or (*Z*)-stilbene) were added. Samples for GC analysis were taken at regular intervals. GC analysis was performed with an HP 6890 series gas chromatograph equipped with an FID detector and an HP-5 GC column (Agilent Technologies). Used catalyst for recycling experiments was obtained from an experiment in which 20 mg instead of 2.0 mg were employed because of difficulties in recovering the small catalyst amount used in the standard experiment. Autoclave reactions were carried out in a stainless steel autoclave (100 mL) with a PTFE inset. The reactor was charged with the same amounts of DMF, (*E*)-stilbene, biphenyl, and STA-12(Co) as described above. A magnetic stirrer was added, the autoclave sealed, purged several times with oxygen and finally pressurized to the desired oxygen pressure. The autoclave was immersed in an oil bath heated at approximately 110 °C so that the internal temperature of the autoclave was 100 °C. After the reaction, the autoclave was cooled to room temperature and carefully vented to prevent loss of material. Product analysis was performed by GC as described above.

Acknowledgements

This study is supported by the Technical University of Denmark. Funding by the Graduate School MP_2T and Haldor Topsøe A/S is gratefully acknowledged. We thank Dr. Gordon M. Pearce (University of St. Andrews) for helpful discussions on the material synthesis and structure of STA-12(Co). Dr. Frank Krumeich and the EMEZ (Electron Microscopy ETH Zurich) are acknowledged for microscope time and recording of the SEM pictures. We thank Hasylab at DESY (Hamburg, Germany) for beamtime and DANSCATT and the European Community—Research Infrastructure Action under the FP6 "Structuring the European Research Area" program (through the Integrated Infrastructure Initiative "Integrating Activity on Synchrotron and Free Electron Laser Science"; contract RII3-CT-2004–506008) for financial support.

[1] *Ullmann's Encyclopedia of Industrial Chemistry*, Wiley-VCH, Weinheim, **2003**.
[2] M. McCoy, M. S. Reisch, A. H. Tullo, J.-F. Tremblay, M. Voith, *Chem. Eng. News* **2009**, *87*, 51–59.
[3] M. Dusi, T. Mallat, A. Baiker, *Catal. Rev. Sci. Eng.* **2000**, *42*, 213–278.
[4] R. Murugavel, H. W. Roesky, *Angew. Chem.* **1997**, *109*, 491–494; *Angew. Chem. Int. Ed. Engl.* **1997**, *36*, 477–479.
[5] A. Corma, H. Garcia, *Chem. Rev.* **2002**, *102*, 3837–3892.
[6] M. D. Hughes, Y. J. Xu, P. Jenkins, P. McMorn, P. Landon, D. I. Enache, A. F. Carley, G. A. Attard, G. J. Hutchings, F. King, E. H. Stitt, P. Johnston, K. Griffin, C. J. Kiely, *Nature* **2005**, *437*, 1132–1135.
[7] M. Turner, V. B. Golovko, O. P. H. Vaughan, P. Abdulkin, A. Berenguer-Murcia, M. S. Tikhov, B. F. G. Johnson, R. M. Lambert, *Nature* **2008**, *454*, 981–983.
[8] P. Lignier, S. Mangematin, F. Morfin, J.-L. Rousset, V. Caps, *Catal. Today* **2008**, *138*, 50–54.
[9] C. Aprile, A. Corma, M. E. Domine, H. Garcia, C. Mitchell, *J. Catal.* **2009**, *264*, 44–53.
[10] F. Loeker, W. Leitner, *Chem. Eur. J.* **2000**, *6*, 2011–2015.
[11] D. Dhar, Y. Koltypin, A. Gedanken, S. Chandrasekaran, *Catal. Lett.* **2003**, *86*, 197–200.
[12] E. Angelescu, R. Ionescu, O. D. Pavel, R. Zavoianu, R. Birjega, C. R. Luculescu, M. Florea, R. Olar, *J. Mol. Catal. A: Chem.* **2010**, *315*, 178–186.
[13] Q. H. Tang, Y. Wang, J. Liang, P. Wang, Q. H. Zhang, H. L. Wan, *Chem. Commun.* **2004**, 440–441.
[14] M. Salavati-Niasari, S. Abdolmohammadi, M. Oftadeh, *J. Coord. Chem.* **2008**, *61*, 2837–2851.
[15] M. V. Patil, M. K. Yadav, R. V. Jasra, *J. Mol. Catal. A: Chem.* **2007**, *277*, 72–80.
[16] M. L. Kantam, B. P. C. Rao, R. S. Reddy, N. S. Sekhar, B. Sreedhar, B. M. Choudary, *J. Mol. Catal. A: Chem.* **2007**, *272*, 1–5.
[17] X. Zhang, C. Zeng, L. Zhang, N. Xu, *Kinet. Catal.* **2009**, *50*, 199–204.
[18] X. H. Lu, Q. H. Xia, S. Y. Fang, B. Xie, B. Qi, Z. R. Tang, *Catal. Lett.* **2009**, *131*, 517–525.
[19] Q. H. Tang, Q. H. Zhang, H. L. Wu, Y. Wang, *J. Catal.* **2005**, *230*, 384–397.
[20] K. M. Jinka, J. Sebastian, R. V. Jasra, *J. Mol. Catal. A: Chem.* **2007**, *274*, 33–41.
[21] X.-Y. Quek, Q. Tang, S. Hu, Y. Yang, *Appl. Catal. A* **2009**, *361*, 130–136.
[22] J. Jiang, R. Li, H. Wang, Y. Zheng, H. Chen, J. Ma, *Catal. Lett.* **2008**, *120*, 221–228.
[23] Z. Opre, T. Mallat, A. Baiker, *J. Catal.* **2007**, *245*, 482–486.
[24] K. P. Lillerud, U. Olsbye, M. Tilset, *Top. Catal.* **2010**, *53*, 859–868.
[25] D. Farrusseng, S. Aguado, C. Pinel, *Angew. Chem.* **2009**, *121*, 7638–7649; *Angew. Chem. Int. Ed.* **2009**, *48*, 7502–7513.
[26] J. Lee, O. K. Farha, J. Roberts, K. A. Scheidt, S. T. Nguyen, J. T. Hupp, *Chem. Soc. Rev.* **2009**, *38*, 1450–1459.
[27] A. U. Czaja, N. Trukhan, U. Mueller, *Chem. Soc. Rev.* **2009**, *38*, 1284–1293.
[28] F. X. Llabrés i Xamena, A. Abad, A. Corma, H. Garcia, *J. Catal.* **2007**, *250*, 294–298.

[29] K. Brown, S. Zolezzi, P. Aguirre, D. Venegas-Yazigi, V. Paredes-Garcia, R. Baggio, M. A. Novak, E. Spodine, *Dalton Trans.* **2009**, 1422–1427.
[30] J. Perles, N. Snejko, M. Iglesias, M. A. Monge, *J. Mater. Chem.* **2009**, *19*, 6504–6511.
[31] K. Leus, I. Muylaert, M. Vandichel, G. B. Marin, M. Waroquier, V. Van Speybroeck, P. Van Der Voort, *Chem. Commun.* **2010**, *46*, 5085–5087.
[32] N. V. Maksimchuk, K. A. Kovalenko, S. S. Arzumanov, Y. A. Chesalov, M. S. Melgunov, A. G. Stepanov, V. P. Fedin, O. A. Kholdeeva, *Inorg. Chem.* **2010**, *49*, 2920–2930.
[33] M. H. Alkordi, Y. Liu, R. W. Larsen, J. F. Eubank, M. Eddaoudi, *J. Am. Chem. Soc.* **2008**, *130*, 12639–12641.
[34] D. Jiang, T. Mallat, D. M. Meier, A. Urakawa, A. Baiker, *J. Catal.* **2010**, *270*, 26–33.
[35] M. Tonigold, Y. Lu, A. Mavrandonakis, A. Puls, R. Staudt, J. Möllmer, J. Sauer, D. Volkmer, *Chem. Eur. J.* **2011**, *17*, 8671–8695.
[36] F. Xamena, O. Casanova, R. G. Tailleur, H. Garcia, A. Corma, *J. Catal.* **2008**, *255*, 220–227.
[37] Y. Wu, L.-G. Qiu, W. Wang, Z.-Q. Li, T. Xu, Z.-Y. Wu, X. Jiang, *Transition Met. Chem.* **2009**, *34*, 263–268.
[38] F. Gándara, A. de Andres, B. Gomez-Lor, E. Gutierrez-Puebla, M. Iglesias, M. A. Monge, D. M. Proserpio, N. Snejko, *Cryst. Growth Des.* **2008**, *8*, 378–380.
[39] S. Bhattacharjee, J.-S. Choi, S.-T. Yang, S. B. Choi, J. Kim, W.-S. Ahn, *J. Nanosci. Nanotechnol.* **2010**, *10*, 135–141.
[40] Y. Lu, M. Tonigold, B. Bredenkoetter, D. Volkmer, J. Hitzbleck, G. Langstein, *Z. Anorg. Allg. Chem.* **2008**, *634*, 2411–2417.
[41] M. Tonigold, Y. Lu, B. Bredenkoetter, B. Rieger, S. Bahnmueller, J. Hitzbleck, G. Langstein, D. Volkmer, *Angew. Chem.* **2009**, *121*, 7682–7687; *Angew. Chem. Int. Ed.* **2009**, *48*, 7546–7550.
[42] S. R. Miller, G. M. Pearce, P. A. Wright, F. Bonino, S. Chavan, S. Bordiga, I. Margiolaki, N. Guillou, G. Ferey, S. Bourrelly, P. L. Llewellyn, *J. Am. Chem. Soc.* **2008**, *130*, 15967–15981.
[43] G. M. Pearce, Ph. D. Thesis, University of St. Andrews (UK), **2009**.
[44] A. C. Larson, R. B. Von Dreele, *General Structure Analysis System (GSAS)*, Los Alamos National Laboratory, USA, **1994**.
[45] M. T. Wharmby, G. M. Pearce, J. P. S. Mowat, J. M. Griffin, S. E. Ashbrook, P. A. Wright, L.-H. Schilling, A. Lieb, N. Stock, S. Chavan, S. Bordiga, E. Garcia, G. Pirngruber, M. Vreeke, L. Gora, unpublished results.
[46] D. Jiang, A. Urakawa, M. Yulikov, T. Mallat, G. Jeschke, A. Baiker, *Chem. Eur. J.* **2009**, *15*, 12255–12262.
[47] P. Shringarpure, A. Patel, *J. Mol. Catal. A* **2010**, *321*, 22–26.
[48] I. Z. Éifer, G. A. Rudova, O. N. Semenikhina, O. M. Bochkareva, *Fibre Chem.* **1981**, *13*, 23–26; 26.
[49] H. K. Lee, C. H. Lam, S. L. Li, Z. Y. Zhang, T. C. W. Mak, *Inorg. Chem.* **2001**, *40*, 4691–4695.
[50] E. Giamello, Z. Sojka, M. Che, A. Zecchina, *J. Phys. Chem.* **1986**, *90*, 6084–6091.
[51] C. Comuzzi, A. Melchior, P. Polese, R. Portanova, M. Tolazzi, *Inorg. Chem.* **2003**, *42*, 8214–8222.
[52] A. F. Holleman, E. Wiberg, *Lehrbuch der Anorganischen Chemie*, 101st ed. De Gruyter, Berlin–New York, **1995**.
[53] J. Sebastian, K. M. Jinka, R. V. Jasra, *J. Catal.* **2006**, *244*, 208–218.
[54] J. Simplicio, R. G. Wilkins, *J. Am. Chem. Soc.* **1967**, *89*, 6092–6095.
[55] F. Miller, J. Simplicio, R. G. Wilkins, *J. Am. Chem. Soc.* **1969**, *91*, 1962–1967.
[56] F. Miller, R. G. Wilkins, *J. Am. Chem. Soc.* **1970**, *92*, 2687–2691.
[57] M. Maeder, H. R. Macke, *Inorg. Chem.* **1994**, *33*, 3135–3140.
[58] H. Furutachi, S. Fujinami, M. Suzuki, H. Okawa, *J. Chem. Soc. Dalton Trans.* **1999**, 2197–2203.
[59] M. Mori, J. A. Weil, *J. Am. Chem. Soc.* **1967**, *89*, 3732–3744.
[60] J. P. S. Mowat, J. A. Groves, M. T. Wharmby, S. R. Miller, Y. Li, P. Lightfoot, P. A. Wright, *J. Solid State Chem.* **2009**, *182*, 2769–2778.

Received: April 20, 2011
Revised: September 12, 2011
Published online: December 12, 2011

